

Metal-insulator transition in $\text{Nd}_{1-x}\text{Eu}_x\text{NiO}_3$: Entropy change and electronic delocalization

Cite as: J. Appl. Phys. **117**, 17C105 (2015); <https://doi.org/10.1063/1.4906434>

Submitted: 17 September 2014 . Accepted: 07 October 2014 . Published Online: 23 January 2015

R. F. Jardim, V. B. Barbeta, S. Andrade, M. T. Escote, F. Cordero, and M. S. Torikachvili



View Online



Export Citation



CrossMark

ARTICLES YOU MAY BE INTERESTED IN

[Room temperature Mott metal-insulator transition and its systematic control in \$\text{Sm}_{1-x}\text{Ca}_x\text{NiO}_3\$ thin films](#)

Applied Physics Letters **97**, 032114 (2010); <https://doi.org/10.1063/1.3467199>

[Correlation between stoichiometry, strain, and metal-insulator transitions of \$\text{NdNiO}_3\$ films](#)

Applied Physics Letters **106**, 092104 (2015); <https://doi.org/10.1063/1.4914002>

[Electronic transitions in strained \$\text{SmNiO}_3\$ thin films](#)

APL Materials **2**, 116110 (2014); <https://doi.org/10.1063/1.4902138>

Applied Physics Reviews
Now accepting original research

2017 Journal
Impact Factor:
12.894



Metal-insulator transition in $\text{Nd}_{1-x}\text{Eu}_x\text{NiO}_3$: Entropy change and electronic delocalization

R. F. Jardim,^{1,a)} V. B. Barbeta,² S. Andrade,¹ M. T. Escote,³ F. Cordero,⁴ and M. S. Torikachvili⁵

¹Instituto de Física, Universidade de São Paulo, CP 66318, São Paulo 05315-970, Brazil

²Departamento de Física, Centro Universitário da FEI, São Bernardo do Campo 09850-901, Brazil

³Centro de Engenharia, Modelagem e Ciências Sociais Aplicadas, Universidade Federal do ABC, Santo André 09210-170, Brazil

⁴CNR-ISC, Istituto dei Sistemi Complessi, Area della Ricerca di Roma - Tor Vergata, Via del Fosso del Cavaliere 100, I-00133 Rome, Italy

⁵Department of Physics, San Diego State University, San Diego, California 92182-1233, USA

(Presented 6 November 2014; received 17 September 2014; accepted 7 October 2014; published online 23 January 2015)

The metal-insulator (MI) phase transition in $\text{Nd}_{1-x}\text{Eu}_x\text{NiO}_3$, $0 \leq x \leq 0.35$, has been investigated through the pressure dependence of the electrical resistivity $\rho(P, T)$ and measurements of specific heat $C_p(T)$. The MI transition temperature (T_{MI}) increases with increasing Eu substitution and decreases with increasing pressure. Two distinct regions for the Eu dependence of dT_{MI}/dP were found: (i) for $x \leq 0.15$, dT_{MI}/dP is nearly constant and ~ -4.3 K/kbar; (ii) for $x \geq 0.15$, dT_{MI}/dP increases with x and it seems to reach a saturation value ~ -6.2 K/kbar for the $x = 0.35$ sample. This change is accompanied with a strong decrease in the thermal hysteresis in $\rho(P, T)$ between the cooling and warming cycles, observed in the vicinity of T_{MI} . The entropy change (ΔS) at T_{MI} for the sample $x = 0$, estimated by using the dT_{MI}/dP data and the Clausius-Clapeyron equation, resulted in $\Delta S \sim 1.2$ J/mol K, a value in line with specific heat measurements. When the Eu concentration is increased, the antiferromagnetic (AF) and the MI transitions are separated in temperature, permitting that an estimate of the entropy change due to the AF/Paramagnetic transition be carried out, yielding $\Delta S_M \sim 200$ mJ/mol K. This value is much smaller than that expected for a $s = 1/2$ spin system. The analysis of $\rho(P, T)$ and $C_p(T)$ data indicates that the entropy change at T_{MI} is mainly due to the electronic delocalization and not related to the AF transition. © 2015 AIP Publishing LLC. [<http://dx.doi.org/10.1063/1.4906434>]

Perovskites of the $R\text{NiO}_3$ family (R = rare-earth, except for $R = \text{La}$) can be regarded as strongly correlated electronic systems and exhibit a metal-insulator (MI) phase transition at a critical temperature T_{MI} , which is a function of the ionic radius of the rare-earth.¹ For Nd and Pr, the MI transition also correlates well in temperature with both the onset of antiferromagnetic (AF) order of the Ni sublattice and a structural rearrangement. The ideal cubic structure is usually distorted and characterized by a tolerance factor $t = d_{R-O} / (\sqrt{2} \cdot d_{Ni-O})$, where d_{Ni-O} and d_{R-O} are the $Ni-O$ and $R-O$ distances, respectively. The decrease of the ionic radius of the R element leads to a more distorted structure, as the NiO_6 octahedra tilt about the $[100]$ axis, and rotate, to fill the voids. The tolerance factor is $t = 1$ for the ideal structure and decreases with increasing distortion.²

T_{MI} is related to the Ni-O-Ni superexchange angle θ (Ref. 3) that decreases from its ideal 180° value with increasing distortion, therefore decreasing the Ni ($3d$) and the O ($2p$) orbital overlap, and favoring the insulating behavior. Neutron diffraction data reveal that the magnetic ground state of these compounds can be described by a $k = (1/2, 0, 1/2)$ spin density wave, associated with an AF ordering of the Ni sublattice.⁴ While the AF transition temperature T_N is

coincident with T_{MI} for $R = \text{Nd}$ and Pr, for other heavier rare-earth elements $T_N < T_{MI}$.

The $(1/2, 0, 1/2)$ propagation vector was initially attributed to an unusual up-up-down-down spin arrangement of the Ni ions, with stacking of ferromagnetic planes coupled antiferromagnetically along the simple cubic $[111]$ direction, due to orbital ordering (OO).⁴ However, soft X-ray resonant scattering experiments performed in NdNiO_3 indicated that the magnetic signal was not consistent with the up-up-down-down spin arrangement, and a non collinear magnetic structure with the absence of OO was proposed.⁵

Neutron and X-ray diffraction measurements on YNiO_3 showed a change in the crystal structure when the MI phase transition takes place. At high temperature, the structure is orthorhombic, and it undergoes a transition to monoclinic below T_{MI} , with the space group changing from $Pbnm$ to $P2_1/n$.⁶ This results in two different Ni-O bond lengths, leading to two distinct Ni sites, and the onset of the electronically insulating behavior. Although this picture has been proposed for the whole series, only recently high-resolution synchrotron X-ray powder diffraction results allowed to extend it to the compound with $R = \text{Nd}$.⁷ When the electronic localization occurs, a charge disproportionation $2\text{Ni}^{3+} \rightarrow \text{Ni}^{3+\delta} + \text{Ni}^{3-\delta}$, and consequently a charge ordered (CO) state, also sets in.⁶ The degree of charge disproportionation δ seems to

^{a)}Electronic mail: rjardim@if.usp.br.

be smaller for the lighter lanthanides, with $\delta \sim 0.2\text{--}0.3$, as in the case for $R = \text{Nd}$.⁷

The proposition of a CO state is still a matter of controversy.^{8,9} In a recent study with smaller rare-earth ions ($R = \text{Eu}, \text{Y}, \text{Lu}$),⁸ the pressure dependence of T_{MI} was interpreted as indicative of an insulating ground state with OO instead of CO. On the other hand, an anelastic spectroscopy study of the MI transition in $\text{Nd}_{1-x}\text{Eu}_x\text{NiO}_3$, $x = 0$ and 0.35, indicated that the elastic anomaly at T_{MI} in NdNiO_3 is not related to the AF transition.⁹ Furthermore, it was argued that the observed steplike stiffening near T_{MI} may be related to the disappearance or freezing out of dynamic Jahn-Teller (JT) distortions through the MI phase transition, where the JT active Ni^{3+} is disproportionated into alternating $\text{Ni}^{3+\delta}$ and $\text{Ni}^{3-\delta}$.⁹

Within this context, it is well established that an external hydrostatic pressure P favors the metallic state in $R\text{NiO}_3$ compounds.^{2,10} Increasing P results in a decrease of the bond lengths and the unit cell volume, driving the atomic parameters toward their ideal values for an undistorted structure.¹¹ Since increasing P favors the metallic state, such an effect may be understood as a decrease in the distortion of the perovskite due to the Ni-O distance shrinking faster than the R-O. However, a different picture for the P effect on the MI phase transition was proposed within the framework of a polaronic model.¹⁰ According to the latter, rather than acting on t , the effect of P is to increase the vibrational frequency of oxygen, and consequently to reduce the activation energy, leading the system back to its metallic state.¹⁰

One difficulty in probing the unusual properties of NdNiO_3 is that the MI and the AF transitions occur at the same temperature, $T_{MI} \sim T_N \sim 200$ K. However, in light of these two transitions being decoupled in Eu-doped $\text{Nd}_{1-x}\text{Eu}_x\text{NiO}_3$ for $x \geq 0.25$, these materials present a viable opportunity for deconvoluting the effects of the structural and magnetic contributions to the electronic behavior. Here, we describe a study of the $\text{Nd}_{1-x}\text{Eu}_x\text{NiO}_3$, $0 \leq x \leq 0.35$, compounds by means of measurements of specific heat $C_P(T)$ and electrical resistivity under pressure $\rho(P, T)$.

Polycrystalline samples of $\text{Nd}_{1-x}\text{Eu}_x\text{NiO}_3$, $0 \leq x \leq 0.35$, were prepared from sol-gel precursors, sintered at $T \sim 1000$ °C, and under oxygen pressures up to 80 bars.^{12,13} X-ray powder diffraction patterns obtained at room temperature for all samples showed only reflections belonging to the desired phase. The temperature dependence of the lattice parameters, obtained from neutron diffraction data, as well as the X-ray data can be found elsewhere.¹⁴ The electrical resistivity measurements $\rho(P, T)$ were performed by using a BeCu piston-cylinder cell, with the temperature ranging from 77 up to 350 K. A mixture of light mineral oil (40%) and n-pentane (60%) was used as the pressure-transmitting medium, and the maximum pressure achieved was ~ 10 kbar. The temperature sweep rates were ~ 2 K/min and ~ 0.5 K/min upon cooling and warming, respectively, and the temperature of the sample was determined with a calibrated type-J thermocouple placed inside of the sample chamber. The P at each T was determined from the change in electrical resistance of a manganese wire.¹⁵ As the internal P changes noticeably with temperature, all the results were corrected in order to account for these

changes. The P values quoted in the figures are the estimated values at T_{MI} upon warming. Specific heat measurements $C_P(T)$ in the T range from 2 to 310 K, upon cooling and warming, were performed with a Physical Property Measurement System (PPMS) from Quantum Design equipped with a superconducting 9 T magnet.

The $\rho(P, T)$ curves for $x = 0$ sample, upon cooling and warming, are displayed in Fig. 1. We first note the occurrence of a large thermal hysteresis ΔT between cooling and warming cycles in the vicinity of T_{MI} , a feature consistent with the first order character of the MI transition. In the temperature interval ΔT , both phases (insulating and metallic) coexist.¹⁶ The cooling curves are essentially coincident and insensitive to P , and the $\rho(T)$ behavior upon warming clearly indicates that the MI phase transition temperature is progressively moving towards lower temperatures with increasing P , favoring the metallic state. ΔT also decreases with increasing P and such a decrease is related to a gradual change in the character of the MI phase transition from first to second order.¹³ This kind of behavior is reminiscent of other ferroelectric perovskites, e.g., BaTiO_3 and PbTiO_3 , which exhibit P induced change in the character of the ferroelectric phase transition.¹⁷

With increasing applied P , a shift of both cooling and warming curves to lower temperatures is observed in the $\rho(P, T)$ curves for the sample with $x = 0.35$, as displayed in Fig. 2. We mention that ΔT is very small at ambient pressure but it increases appreciably under P , the opposite behavior found in NdNiO_3 . Similarly to the results for NdNiO_3 , applied P favors the metallic state, although in this case both curves are shifted to lower temperatures, as observed in $\text{Sm}_{0.5}\text{Nd}_{0.5}\text{NiO}_3$.¹⁰

Increasing Eu content results in an increase in T_{MI} , as displayed in Table I. The T_{MI} values were obtained from the inflection points of the $\rho(T)$ warming curves and ΔT_0 , obtained at ambient pressure, decreases with increasing Eu content. In fact, ΔT_0 is suppressed upon substitution of Eu for Nd being reduced to nearly zero for $x = 0.35$, further suggesting that a lattice distortion promoted by the Eu substitution drives the MI phase transition from first towards second order.

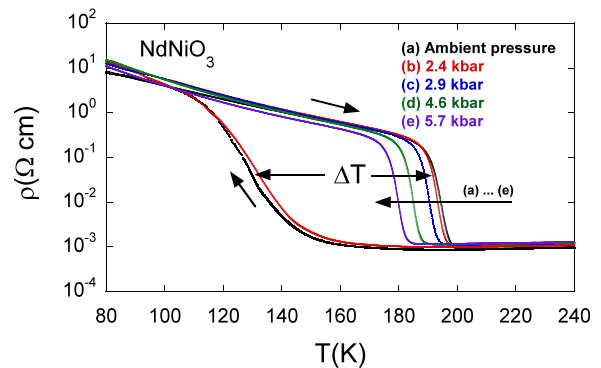


FIG. 1. Temperature dependence of the electrical resistivity of NdNiO_3 for five different applied pressures. The interval ΔT is the temperature difference between the inflection points of the MI transitions upon cooling and warming.

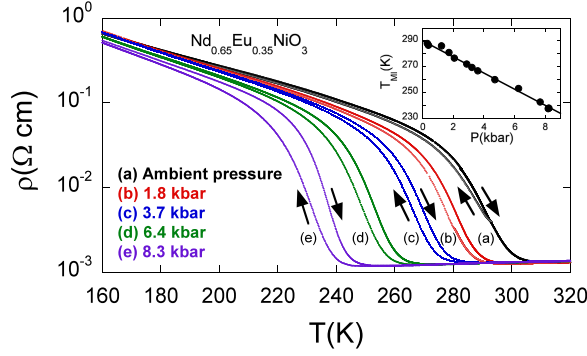


FIG. 2. Temperature dependence of the electrical resistivity of polycrystalline $\text{Nd}_{0.65}\text{Eu}_{0.35}\text{NiO}_3$ for five different applied pressures. The upper inset shows T_{MI} vs. P . The solid line shown in the inset is a linear fit to the data.

TABLE I. Ambient pressure MI transition temperature (T_{MI}), thermal hysteresis width (ΔT_0), and $-dT_{MI}/dP$ in $\text{Nd}_{1-x}\text{Eu}_x\text{NiO}_3$ compounds.

x	T_{MI} (K)	ΔT_0 (K)	$-dT_{MI}/dP$ (K/kbar)
0	197	60	4.29
0.10	219	44	4.42
0.15	229	28	4.44
0.25	259	8	5.46
0.30	274	6	6.10
0.35	297	~ 0	6.23

The pressure derivatives dT_{MI}/dP were extracted from the $\rho(P, T)$ data upon warming for all compositions. The behavior of T_{MI} versus P for all samples was fit by linear regression (see inset of Fig. 2), and the dT_{MI}/dP versus x data are displayed in Table I. Two different regimes for the Eu dependence of dT_{MI}/dP : (i) for $x \leq 0.15$, dT_{MI}/dP is nearly constant and ~ -4.5 K/kbar; (ii) for $x > 0.15$, the magnitude of dT_{MI}/dP increases with x and it seems to approach a saturation value ~ -6.2 K/kbar for the $x=0.35$ sample. The value obtained for the $x=0$ sample (~ -4.3 K/kbar) is in excellent agreement with $dT_{MI}/dP \sim -4.2$ K/kbar found elsewhere,¹⁸ lending further credence to our results.

In light of the first order character of the MI transition, it is important to estimate the change in entropy ΔS by using the Clausius-Clapeyron equation $\Delta S = \Delta V (dP/dT_{MI})$, where ΔV is the molar volume change at T_{MI} . The unit cell volume (V_{cell}) is obtained from the unit cell parameters, and the molar volume V expressed as $V = N_A V_{cell}/Z$, where N_A is the Avogadro number and Z is the number of formula units in the unit cell. Using $Z=4$ for $\text{Nd}_{1-x}\text{Eu}_x\text{NiO}_3$, $0 \leq x \leq 0.35$, and taking the values of V_{cell} from Ref. 15, $V \sim 33.3$ and ~ 33.1 cm^3/mol for samples with $x=0$ and 0.30 , respectively, were obtained. Substituting these values in the Clausius-Clapeyron equation, and considering that $\Delta V/V_0 \sim 0.220\%$ and 0.180% for $x=0$ and $x=0.30$, respectively,¹⁴ the values of the entropy change ΔS_C across the transition ~ 1.7 and ~ 1.0 J/mol K are obtained. The calculated values of ΔS_C for the whole series are displayed in Table II, and they reflect the expected entropy change due to the abrupt jump in the volume at T_{MI} , independently of its origin. This entropy change can be ascribed to different factors like the

TABLE II. Normalized volume contraction ($\Delta V/V_0$), volume contraction (ΔV), rate of change of T_{MI} with pressure (dT_{MI}/dP), and calculated entropy change (ΔS_C) for different Eu content (x).

x	$\Delta V/V_0(\%)$	$\Delta V (10^{-8} \text{ m}^3/\text{mol})$	$-dT_{MI}/dP$ (K/kbar)	ΔS_C (J/mol K)
0	0.220	7.32	4.3	1.7
0.10	0.207	6.86	4.4	1.6
0.15	0.200	6.64	4.5	1.5
0.25	0.187	6.18	5.5	1.1
0.30	0.180	5.96	6.1	1.0
0.35	0.173	5.73	6.3	0.9

electron delocalization and the antiferromagnetic/paramagnetic transition.

The data shown in Table II indicate that ΔS_C decreases progressively with increasing Eu content. On the other hand, this estimate methodology starts to fail when the character of the transition changes from first to second order, as the Clausius-Clapeyron equation is no longer valid. For a second order phase transition, dT_{MI}/dP is related to the specific heat anomaly (ΔC_p) through the Ehrenfest relation. In this case, $\Delta\beta = -(\Delta C_p/V_{mol}T_{MI})(dT_{MI}/dP)$, where $\Delta\beta$ is the change in the volumetric thermal expansion coefficient, and V_{mol} is the molar volume.¹⁹

Values of ΔS_C at the MI transition shown in Table II are consistent with other results from the literature. For example, ΔS values, determined by differential scanning calorimetry DSC, for NdNiO_3 were $\Delta S \sim 1.3$ and ~ 1.7 J/mol K, in Refs. 15 and 20, respectively. As pointed out in Refs. 15 and 20, ΔS at the MI transition is much smaller than the theoretical entropy increase ΔS_M expected for the AF to paramagnetic transition of a spin $s=1/2$ ion ($\Delta S_M = R \ln(2s+1) \sim 5.8$ J/mol K). However, it is worth to note that this entropy change is obtained only when the material undergoes a magnetic transition from a completely ordered state to a disordered one. Usually, the experimental values are reduced by thermal fluctuations, and are frequently lower than the expected upper limit.

The values of ΔS were also obtained from specific heat measurements. A background contribution to $C_p(T)$ has been subtracted from the original curves and the resulting specific heat ($C_R(T)$) is displayed in Fig. 3. The subtraction

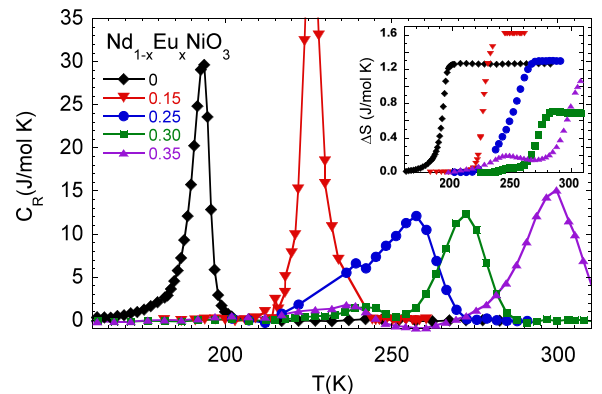


FIG. 3. Residual specific heat (C_R) for $\text{Nd}_{1-x}\text{Eu}_x\text{NiO}_3$ compounds after subtracting the lattice contribution, as described in the text. The inset shows the respective entropy change (ΔS). Solid lines are a guide to the eye.

was performed by excluding the region close to the phase transition in the warming cycle, and fitting the background data to a smooth base-line. The $C_R(T)$ curve for the $x=0$ sample displays a very sharp peak at $T_{MI}=T_N \sim 195$ K. However, the partial substitution of Nd by Eu results in a separation of the two transitions, as seen in the $x=0.25$ sample, which exhibits two peaks: one at $T \sim 240$ K, related to the AF transition, and the other one at $T \sim 270$ K, due to the MI transition. The separation in temperature of the two transitions is even more evident in the $x=0.35$ sample, where the two peaks are completely resolved in spite of some broadening in comparison with the $x=0$ sample.

From the specific heat $C_R(T)$ curves, we obtained the experimental ΔS associated with the MI phase transition. These results are shown in the inset of Fig. 3 and two important features are observed: (i) for Eu concentration $x < 0.25$, the two transitions (MI and AF) occur simultaneously, $\Delta S \sim 1.4$ J/mol K for the $x=0$, increasing slightly with x , and the change of ΔS across the transition is sharp; (ii) for $x > 0.25$, the change of ΔS across the transition is smoother, and much less pronounced when compared to the $x=0.15$ sample.

The entropy change ΔS_M related to the AF transition may be obtained directly in systems where $T_{MI} \neq T_N$. By inspecting the data displayed in the inset of Fig. 3, the magnetic entropy change for the sample with $x=0.35$ was estimated to be $\Delta S_M \sim 200$ mJ/mol K. Again, this is much smaller than the full $R \ln(2)$ value of $\Delta S_M = 5.8$ J/mol K but in line with other experimental values, as low as 190 mJ/mol K, and as high as 754 mJ/mol K found in GdNiO₃ and DyNiO₃, respectively.²¹ Therefore, the entropy change at T_{MI} for the $x=0$ sample may be attributed mainly to the electronic delocalization, i.e., the magnetic entropy change due to the antiferromagnetic/paramagnetic transition is quite small.

It is somewhat puzzling that ΔS_M near T_N is so small. Within this context, several scenarios need to be considered. First, a small value of ΔS may be due to a depopulation of the AF states with increasing temperature below T_N . However, this argument fails when the temperature dependence of the Ni saturation moment in NdNiO₃ and PrNiO₃ is taken into account.²² The neutron diffraction data of Ref. 22 indicate that $\sim 90\%$ of the saturation moment of the Ni sublattice in NdNiO₃ is already established at ~ 150 K, which is inconsistent with the small entropy change at $T_N \sim 200$ K. Another possible reason would be the existence of short-range order AF correlations in a wide range of temperature,

including the temperature range close to T_{MI} . Since the background contribution has been obtained fitting the specific heat data and excluding the region in the vicinity of T_{MI} , the existence of short ranged AF correlations above and below T_N is not accounted for in the process. However, the presence of short-range magnetic correlations above T_{MI} has been already observed in NdNiO₃,²³ lending credence to this possibility. We finally consider the X-ray Absorption Spectroscopy (XAS) measurements performed in RNiO₃ ($R = \text{Nd, Pr, Eu, Y}$) indicating the presence of two different Ni sites coexisting in the metallic state of these nickelates.²³ These two Ni sites, owing different Ni magnetic moments, are responsible for the strange AF arrangement in the insulating phase. In addition to this, recent XAS measurements in YNiO₃ under P have provided clear evidence that the MI transition is bandwidth-driven and not related to a sudden modification in the local geometry of the NiO₆ octahedra.²⁴ These results corroborate our findings that the magnetic ordering of the Ni ions has little effect on the MI transition and the entropy released at T_{MI} is mainly due to the electronic delocalization.

The authors gratefully acknowledge support from Brazil's agencies FAPESP (Grant No. 2013/07296-2), CNPq, CAPES, and USA's NSF Grant No. DMR-0805335 (MST).

¹G. Catalan, *Phase Transitions* **81**, 729 (2008).

²M. L. Medarde, *J. Phys.: Condens. Matter* **9**, 1679 (1997).

³J. L. García-Muñoz *et al.*, *Phys. Rev. B* **46**, 4414 (1992).

⁴J. L. García-Muñoz *et al.*, *Europhys. Lett.* **20**, 241 (1992).

⁵V. Scagnoli *et al.*, *Phys. Rev. B* **73**, 100409(R) (2006).

⁶J. A. Alonso *et al.*, *Phys. Rev. Lett.* **82**, 3871 (1999).

⁷J. L. García-Muñoz *et al.*, *Phys. Rev. B* **79**, 134432 (2009).

⁸J. G. Cheng *et al.*, *Phys. Rev. B* **82**, 085107 (2010).

⁹F. Cordero *et al.*, *Phys. Rev. B* **84**, 125127 (2011).

¹⁰J. S. Zhou *et al.*, *Phys. Rev. B* **61**, 4401 (2000).

¹¹M. Amboage *et al.*, *J. Phys.: Condens. Matter* **17**, S783 (2005).

¹²M. T. Escote *et al.*, *J. Solid State Chem.* **151**, 298 (2000).

¹³V. B. Barbeta *et al.*, *J. Appl. Phys.* **109**, 07E115 (2011).

¹⁴M. T. Escote *et al.*, *J. Phys.: Condens. Matter* **18**, 6117 (2006).

¹⁵J. D. Thompson, *Rev. Sci. Instrum.* **55**, 231 (1984).

¹⁶X. Granados *et al.*, *Phys. Rev. B* **48**, 11666 (1993).

¹⁷R. Ramírez *et al.*, *Phys. Rev. B* **42**, 2604 (1990).

¹⁸X. Obradors *et al.*, *Phys. Rev. B* **47**, 12353 (1993).

¹⁹J. A. Souza *et al.*, *Phys. Rev. Lett.* **94**, 207209 (2005).

²⁰J. Pérez-Cacho *et al.*, *J. Phys.: Condens. Matter* **11**, 405 (1999).

²¹J. A. Alonso *et al.*, *Chem. Mater.* **11**, 2463 (1999).

²²J. L. García-Muñoz *et al.*, *Phys. Rev. B* **50**, 978 (1994).

²³C. Piamonteze *et al.*, *Phys. Rev. B* **71**, 012104 (2005).

²⁴A. Y. Ramos *et al.*, *Phys. Rev. B* **85**, 045102-1 (2012).